Electronic Supplementary Material (ESI) for Journal of Materials Chemistry C.

SUPORTING INFORMATION

Multifunctional Properties of D-A Luminophores Based on Acenaphtopyrido[2,3-b]pyrazine Core: Photophysics, Photochemistry, and Efficient Solution-Processed OLEDs

Welisson de Pontes Silva,[†ab] Nícolas Oliveira Decarli,[†ab] Leandro Espíndola[c], Karol Erfurt,[a] Agata Blacha-Grzechnik,[ab] Piotr Pander,[ab*] Mieczyslaw Lapkowski,[abd*] and Przemyslaw Data[e*]

*Corresponding author;

[†]These authors contributed equally to the experimental work.

[a] *Faculty of Chemistry, Silesian University of Technology, M. Strzody 9, 44-100, Gliwice, Poland. E-mail: mieczyslaw.lapkowski@polsl.pl; piotr.pander@polsl.pl.*

[b] *Centre for Organic and Nanohybrid Electronics, Silesian University of Technology, Konarskiego 22b, 44-100 Gliwice, Poland.*

[c] *Departament of Chemistry, Universidade Estadual de Ponta Grossa, Campus Central - Praça Santos Andrade, 01 - Centro, Ponta Grossa - PR, CEP 84010-330, Brazil.*

[d] *Centre of Polymer and Carbon Materials, Polish Academy of Sciences, M. Curie-Skłodowska 34, Zabrze 41-819, Poland. E-mail: mieczyslaw.lapkowski@pan.pl*

[e] *Łódź University of Technology, Department of Chemistry, Stefana Żeromskiego 114, Łódź 90-543, Poland. E-mail: przemyslaw.data@p.lodz.pl*

Table of contents

1. General Remarks 3
2. Materials 3
3. Photophysics 3
4. Theoretical calculations 4
5. Cyclic Voltammetry 4
6. Singlet oxygen experiments 4
7. Device Fabrication and Characterization 5
8. Synthetic procedures and spectroscopy data 6
9. NMR spectra 10
10. Additional theoretical data 19
11. Additional cyclic voltammetry data 21
12. Additional photophysical data 22
13. Singlet oxygen generation 28
14. Aggregation study 29
15. OLED devices additional data 31
16. Thermogravimetric analysis (TGA) 32
17. References 33

1. General Remarks

All the reagents were obtained from commercial sources and used without further purification. The N-C coupling reactions were accomplished under Ar atmosphere. The organic solvents were of commercial grade quality. In general, all the compounds were purified by column chromatography on silica gel (60–200 mesh), and recrystallization from analytical grade solvents. The purity of the sample was checked by thin-layer chromatography (Merck Kieselgel 60F254). ^{1}H and ^{13}C NMR spectra were recorded on a Varian Unity Inova spectrometer (^{1}H NMR: 300 MHz, ^{13}C NMR: 75MHz) using tetramethylsilane (δ = 0 ppm) as an internal. High-resolution mass spectra (HRMS) were obtained on a Waters Xevo G2 Q-TOF mass spectrometer.

2. Materials

10-Bromoacenaphtho[1,2-b]pyrido[2,3-e]pyrazine (**NQPy-Br**) was prepared according to the literature procedure.[1] 9-dimethyl-9,10-dihydroacridine (**DMAC**) and 9,9-diphenyl-9,10-dihydroacridine (**DPAC**) were prepared according to the procedures in literature.[2] Commercial reagents were purchased from Sigma-Aldrich, TCI, or Alfa Aesar and used as received.

3. Photophysics

UV-vis spectra were recorded on a Shimadzu UV-2550 spectrophotometer. Steady state emission spectra were recorded on a HAMAMATSU C11347-01 spectrometer with an integrating sphere and Jobin Yvon Horiba Fluorolog 3, with solvent studies performed in clean 1 cm path-length photoluminescence cuvettes (Arieka Cells). Photoluminescence spectra were calibrated for detector efficiency using company supplied, instrument specific calibration files. Solid state samples were prepared with 1% w/w ratio emitters in Zeonex polymer host or 10% CBP host on clean sapphire disc substrates. Phosphorescence, prompt fluorescence (PF), and delayed fluorescence (DF) spectra and decays were recorded using nanosecond gated luminescence and lifetime measurements (from 400 ps to 1 s) using the third harmonics of a high energy pulsed DPSS laser emitting at 355 nm (Q-Spark A50-TH-RE). Emission was focused onto a spectrograph and detected on a sensitive gated iCCD camera (Stanford Computer

Optics) having sub-nanosecond resolution. PF/DF time-resolved measurements were performed by exponentially increasing gate and integration times. Temperature dependent experiments were conducted using an helium cryocooler (Janis Research) under a vacuum.

4. Theoretical calculations

All theoretical calculations were performed using Schrodinger® software. Density functional theory (DFT) calculations were used to obtain the optimized molecular geometries of all compounds. To calculate the frontier molecular orbitals (FMOs) with HOMO-LUMO spatial distributions we used the hybrid functional B3LYP along with the 6-31G** basis set. Excited state calculations to estimate the energies of S_1, T_1 and T_2 used time-dependent (TD) DFT at B3LYP/6-31G** level and the Tamm-Dancoff approximation (TDA).

For the natural transitions orbitals (NTOs) HONTO and LUNTO for excited states S_1, T_1 and T_2 we used the long-range corrected functional LC-ωPBE along with the 6-31G basis set as previously reported.[1] Solvent effects were accounted for with the polarizable continuum model using parameters for toluene. Excited states calculations employed the Tamm-Dancoff approximation (TDA).

5. Cyclic Voltammetry

Electrochemical measurements were performed using a potentiostat PGSTAT100 AUTOLAB with 0.1 M Bu_4NBF_4 (99%, Sigma Aldrich, dried) in dichloromethane (CHROMASOLV®, 99.9% Sigma Aldrich). Solutions were purged with argon prior to measurement. Electrodes: working (Pt disc 1 mm of diameter), counter (Pt wire), reference (Ag/AgCl calibrated against ferrocene).

6. Singlet oxygen experiments

Singlet oxygen experiments were carried out in a quartz cuvette (Hellma Analytics) with 10 mm path using 0.016 mM DCM solutions of photosensitizers and 0.13 mM of tetraphenylcyclopentadienone (TPCPD) as the specific singlet oxygen trap. We monitor temporal changes in absorbance of TPCPD at λ = 510 nm while using the irradiation beam, λ = 445 nm, with *ca*. 0.5 cm^2 cross section in perpendicular configuration to the

UV-Vis spectrometer optical path. The diode laser with the emission wavelength of 445 nm (Oxxius 100 mW model LBX-445- 100-CSB-PP) working at 20 mW was applied as a source of light. The equation used to calculate the singlet oxygen formation (ϕ_Δ) was:

$$\Phi_{\boldsymbol{\Delta}} = \Phi_{\boldsymbol{PN}} . \frac{\boldsymbol{k_i}}{\boldsymbol{k_{PN}}} . \frac{\boldsymbol{\alpha_{PN}}}{\boldsymbol{\alpha_i}}.$$

Where $\boldsymbol{\phi_\Delta}$ is the quantum yield of singlet oxygen formation, $\boldsymbol{\phi_{PN}}$ is the singlet oxygen quantum yield for phenalenone (PN) (0.95 in DCM)[3,4], $\mathbf{k_i}$ is the slope of temporal change in absorbance of TPCPD, $\mathbf{k_{PN}}$ is the slope of temporal change in absorbance of TPCPD and $\boldsymbol{\alpha_i}$ is a function of absorbance at 445 nm, $\alpha = (1 - 10^{-A})$.

7. Device Fabrication and Characterization

OLEDs have been fabricated on pre-cleaned, patterned indium-tin-oxide (ITO) coated glass substrates with a sheet resistance of 20 Ω/sq and ITO thickness of 100 nm. PEDOT:PSS (Al4083 from Heraeus) {poly(3,4-ethylenedioxythiophene) polystyrene sulfonate} was used as a Hole Injection Layer (HIL) and Hole Transport Layer (HTL). TPBi {2,2',2"-(1,3,5-benzinetriyl)-tris(1-phenyl-1-*H*-benzimidazole)} was introduced as an Electron Transport Layer (ETL). Lithium fluoride (LiF) and aluminium were used as the cathode. Organic semiconductors and aluminium were deposited at a rate of 1 Å s^{-1}, and the LiF layer was deposited at 0.1 Å s^{-1}. CBP {4,4′-bis(*N*-carbazolyl)-1,1′-biphenyl}, was used as host for all emitters. All materials were purchased from Sigma Aldrich or Lumtec and were purified by temperature-gradient sublimation in a vacuum. PEDOT:PSS layer was prepared on an ITO coated glass substrate by spin coating of the solution at 4000 rpm and 45 s with 15 minutes of annealing treatment at 120 ^{0}C after deposition. The emissive layers were prepared by spin-coating of solution of 95:5 v/v of chloroform and chlorobenzene with 10% of emitter compounds in CBP (HOST) at 4000 rpm and 45 s. All other molecules and cathode layers were thermally evaporated using a Kurt J. Lesker NANO 36^{TM} evaporation system under pressure of 10^{-7} mbar without breaking the vacuum. The sizes of pixels were 4 mm^2, 8 mm^2 and 16 mm^2. The characteristics of the devices were recorded using a 6-inch integrating sphere (Labsphere) connected to a Source Meter Unit and Ocean Optics USB4000 spectrometer.

8. Synthetic procedures and spectroscopy data

10-bromoacenaphtho[1,2-b]pyrido[2,3-e]pyrazine (**NQPy-Br**)

A mixture of acenaphthylene-1,2-dione (1.00 g; 5.48 mmol) and 5-bromopyridine-2,3-diamine (1.08 g; 5.76 mmol) were refluxed in 30 ml of glacial acetic acid for 24h. After the reaction was completed, the reaction mixture was filtrated and washed with water and methanol. The solid was dissolved in 100 ml of chloroform and washed tree times with sodium hydroxide solution (1 M) and water. The organic layer was separated and dried with $MgSO_4$. The solvent was evaporated to give the compound **NQPy-Br** in 73% of yield. **^{1}H NMR** (300 MHz, $CDCl_3$) δ 9.11 (d, *J* = 2.4 Hz, 1H), 8.68 (d, *J* = 2.4 Hz, 1H), 8.52 (d, *J* = 7.0 Hz, 1H), 8.40 (d, *J* = 6.9 Hz, 1H), 8.19 – 8.14 (m, 2H), 7.90 – 7.84 (m, 2H). **^{13}C NMR** (75 MHz, $CDCl_3$) δ 157.2, 155.6, 153.3, 149.1, 139.8, 137.4, 136.8, 130.9, 130.53, 130.50, 130.4, 129.9, 129.1, 128.8, 123.6, 122.8, 119.9.

***General procedures to Buchwald-Hartwig Cross Coupling Reaction* in the NQPy-Br core**

To a Schlenk tube equipped with a reflux condenser was added a mixture of compounds **NQPy-Br** (0.299 mmol), the respective aryl amine (0.389 mmol), *t*-BuONa (0.72 mmol), $Pd_2(dba)_3$ (0.0089 mmol), $[(t\text{-}Bu)_3PH]BF_4$ (0.018 mmol) and 10 mL of degasified toluene. The mixture was stirred at 110 °C for 24h under argon atmosphere. After completed reaction the mixture was filtered through a plug of celite and washed with dichloromethane. The solvents were evaporated, and the residue was purified by column chromatography using dichloromethane as eluent.

10-(acenaphtho[1,2-b]pyrido[2,3-e]pyrazin-10-yl)-10H-phenothiazine (**NQPy-PTZ**)

Yellow solid (73 %). **^{1}H NMR** (300 MHz, $CDCl_3$) δ/ppm: 9.03 (d, *J* = 2.9 Hz, 1H), 8.52 (d, *J* = 6.4 Hz, 1H), 8.40 (d, *J* = 6.6 Hz, 1H), 8.20 (d, *J* = 2.9 Hz, 1H), 8.15 (dd, *J* = 7.9, 4.1 Hz, 2H), 7.87 (ddd, *J* = 8.3, 7.0, 5.2 Hz, 2H), 7.42 (dd, *J* = 7.7, 1.2 Hz, 2H), 7.30 (m, 3H), 7.25 – 7.16 (m, 3H). **^{13}C NMR** (75 MHz, 1,1,2,2-Tetrachloroethane-d_2) δ 153.4, 153.3, 145.6, 145.1, 139.7, 138.6, 134.9, 134.8, 129.28, 128.8, 128.2, 128.1, 127.9, 127.5, 127.0, 126.8, 126.5, 125.7, 125.1, 123.6, 121.0, 120.8, 120.6, 118.3. **HRMS**: m/z calcd for $C_{29}H_{16}N_4S$ $(M+H)^+$: 453.1174; found: 453.1175.

10-(acenaphtho[1,2-b]pyrido[2,3-e]pyrazin-10-yl)-10H-phenoxazine (**NQPy-PXZ**)

Red solid (89 %). **^{1}H NMR** (300 MHz, $CDCl_3$) δ/ppm: 9.11 (d, *J* = 2.6 Hz, 1H), 8.65 (d, *J* = 2.6 Hz, 1H), 8.61 (d, *J* = 7.0 Hz, 1H), 8.47 (d, *J* = 7.0 Hz, 1H), 8.22 (dd, *J* = 8.1, 2.0 Hz, 2H), 7.93 (dt, *J* = 8.2, 7.1 Hz, 2H), 6.82 – 6.72 (m, 4H), 6.65 (ddd, *J* = 7.9, 7.0, 2.0 Hz, 2H), 6.11 (dd, *J* = 8.0, 1.3 Hz, 2H). **^{13}C NMR** (75 MHz, 1,1,2,2-Tetrachloroethane-d_2) δ 158.9, 156.8, 156.2, 151.0, 145.4, 141.9, 138.8, 138.5, 136.9, 134.8, 132.2, 131.9, 131.8, 131.4, 130.6, 130.4, 124.9, 124.5, 124.0, 117.5, 114.9. **HRMS**: m/z calcd for $C_{29}H_{16}N_4O$ $(M+H)^+$: 437.1402; found: 437.1400.

*10-(9,9-dimethylacridin-10(9H)-yl)acenaphtho[1,2-b]pyrido[2,3-e]pyrazine (**NQPy-DMAC**)*

Yellow solid (87 %). **^{1}H NMR** (300 MHz, $CDCl_3$) δ/ppm: 9.09 (d, *J* = 2.6 Hz, 1H), 8.67 (d, *J* = 2.6 Hz, 1H), 8.62 (d, *J* = 6.7 Hz, 1H), 8.47 (d, *J* = 6.8 Hz, 1H), 8.22 (dd, *J* = 8.0, 2.4 Hz, 2H), 7.97 – 7.87 (m, 2H), 7.54 (dd, *J* = 6.1, 3.2 Hz, 2H), 7.06 – 6.99 (m, 4H), 6.44 (dd, *J* = 6.2, 3.3 Hz, 2H), 1.75 (s, 6H). **^{13}C NMR** (75 MHz, $CDCl_3$) δ/ppm: 157.4, 155.4, 155.4, 155.3, 149.7, 140.5, 139.9, 138.0, 137.5, 137.2, 131.3, 131.1, 130.7, 130.5, 130.4, 130.1, 129.1, 128.9, 126.6, 125.5, 123.6, 122.7, 121.8, 114.6, 36.2, 30.8. **HRMS**: m/z calcd for $C_{32}H_{22}N_4$ $(M+H)^+$: 463.1923; found: 463.1923.

*10-(9,9-diphenylacridin-10(9H)-yl)acenaphtho[1,2-b]pyrido[2,3-e]pyrazine (**NQPy-DPAC**)*

Yellow solid (91 %). **^{1}H NMR** (300 MHz, DMSO) δ/ppm: 8.66 – 8.53 (m, 2H), 8.44 (dd, *J* = 22.3, 4.6 Hz, 4H), 8.01 (dd, *J* = 14.4, 6.9 Hz, 4H), 7.41 – 7.30 (m, 6H), 7.16 (t, *J* = 7.6 Hz, 2H), 7.02 (t, *J* = 7.5 Hz, 2H), 6.94 (d, *J* = 7.1 Hz, 4H), 6.85 (d, *J* = 7.8 Hz, 2H), 6.67 (d, *J* = 8.2 Hz, 2H). **^{13}C NMR** (75 MHz, $CDCl_3$) δ/ppm: 157.4, 155.5, 155.0, 149.6, 145.9, 141.9, 139.0, 137.8, 137.5, 136.9, 131.8, 131.3, 130.9, 130.5, 130.4, 130.2, 129.1, 128.9, 127.9, 127.2, 126.7, 123.7, 122.7, 121.5, 115.1. **HRMS**: m/z calcd for $C_{42}H_{26}N_4$ $(M+H)^+$: 587.2236; found: 587.2233.

*10-(9H-carbazol-9-yl)acenaphtho[1,2-b]pyrido[2,3-e]pyrazine (**NQPy-CBZ**)*

Yellow solid (44 %).**^{1}H NMR** (300 MHz, $CDCl_3$) δ/ppm: 9.34 (d, *J* = 2.6 Hz, 1H), 8.70 (d, *J* = 2.6 Hz, 1H), 8.51 (d, *J* = 6.9 Hz, 1H), 8.36 (d, *J* = 6.9 Hz, 1H), 8.22 – 8.01 (m, 4H), 7.82 (td, *J* = 8.4, 7.1 Hz, 2H), 7.53 (d, *J* = 8.2 Hz, 2H), 7.45 – 7.36 (m, 2H), 7.36 – 7.24 (m, 2H). **^{13}C NMR** (75 MHz, $CDCl_3$) δ/ppm: 157.3, 155.9, 151.1, 149.2, 140.5, 137.6, 136.8, 134.8, 134.2, 131.2, 130.8, 130.6, 130.5, 130.2, 129.2, 128.9, 126.7, 124.3, 123.7, 122.9, 121.3, 120.8, 109.6. **HRMS**: m/z calcd for $C_{29}H_{17}N_4$ $(M+H)^+$: 421.1453; found: 421.1454.

*N,N-diphenylacenaphtho[1,2-b]pyrido[2,3-e]pyrazin-10-amine (**NQPy-DPA**)*

Yellow solid (93 %).**^{1}H NMR** (300 MHz, $CDCl_3$) δ/ppm: 8.94 (d, *J* = 2.9 Hz, 1H), 8.48 (d, *J* = 7.0 Hz, 1H), 8.34 (d, *J* = 7.0 Hz, 1H), 8.13 (dd, *J* = 8.2, 5.2 Hz, 2H), 7.93 (d, *J* = 2.9 Hz, 1H), 7.85 (td, *J* = 8.2, 7.1 Hz, 2H), 7.39 (tt, *J* = 4.0, 2.0 Hz, 4H), 7.28 (d, *J* = 1.3 Hz, 2H), 7.26 – 7.18 (m, 4H). **^{13}C NMR** (75 MHz, $CDCl_3$) δ/ppm: 155.4, 154.4, 148.6, 146.2, 145.1, 137.5, 136.7, 131.9, 131.4, 130.1, 130.1, 130.0, 129.6, 129.0, 128.7, 125.6, 125.2, 124.5, 122.7, 122.1. **HRMS**: m/z calcd for $C_{29}H_{19}N_4$ $(M+H)^+$: 423.1610; found: 423.1611.

*10-(10,11-dihydro-5H-dibenzo[b,f]azepin-5-yl)acenaphtho[1,2-b]pyrido[2,3-e]pyrazine (**NQPy-DDA**)*

Yellow solid (90 %).**^{1}H NMR** (300 MHz, $CDCl_3$) δ/ppm: 8.68 (d, *J* = 3.1 Hz, 1H), 8.43 (d, *J* = 7.0 Hz, 1H), 8.31 (d, *J* = 7.0 Hz, 1H), 8.08 (t, *J* = 8.6 Hz, 2H), 7.81 (dd, *J* = 15.0, 6.8 Hz, 2H), 7.54 (dd, *J* = 7.0, 2.2 Hz, 3H), 7.36 (qd, *J* = 6.1, 3.7 Hz, 6H), 3.07 (s, 4H). **^{13}C NMR** (75 MHz, $CDCl_3$) δ/ppm: 155.3, 153.1, 145.5, 144.4, 142.1, 137.9, 137.5, 136.4, 132.1, 131.6, 131.5, 129.9, 129.7, 129.11 129.0, 128.9, 128.5, 128.2, 127.8, 122.2, 121.8, 115.0, 30.7. **HRMS**: m/z calcd for $C_{31}H_{21}N_4$ $(M+H)^+$: 449.1766; found: 449.1761.

*10-(5H-dibenzo[b,f]azepin-5-yl)acenaphtho[1,2-b]pyrido[2,3-e]pyrazine (**NQPy-IMD**)*

Yellow solid (48 %).**^{1}H NMR** (300 MHz, $CDCl_3$) δ/ppm: 8.41 (dd, *J* = 7.0, 0.5 Hz, 1H), 8.35 (d, *J* = 3.1 Hz, 1H), 8.29 (d, *J* = 7.1 Hz, 1H), 8.07 (t, *J* = 8.5 Hz, 2H), 7.80 (ddd, *J* = 8.2, 7.0, 6.2 Hz, 2H), 7.65 – 7.58 (m, 4H), 7.55 – 7.44 (m, 4H), 7.24 (dd, *J* = 2.8, 1.8

Hz, 1H), 6.89 (s, 2H). **^{13}C NMR** (75 MHz, $CDCl_3$) δ/ppm: 155.2, 153.1, 145.3, 144.7, 141.5, 141.5, 137.3, 136.4, 135.9, 132.0, 131.5, 130.8, 130.6, 130.5, 129.9, 129.7, 129.5, 129.0, 128.8, 128.5, 128.0, 122.2, 121.7, 114.6. **HRMS**: m/z calcd for $C_{31}H_{19}N_4$ $(M+H)^+$: 447.1610; found: 447.1610.

9. NMR spectra

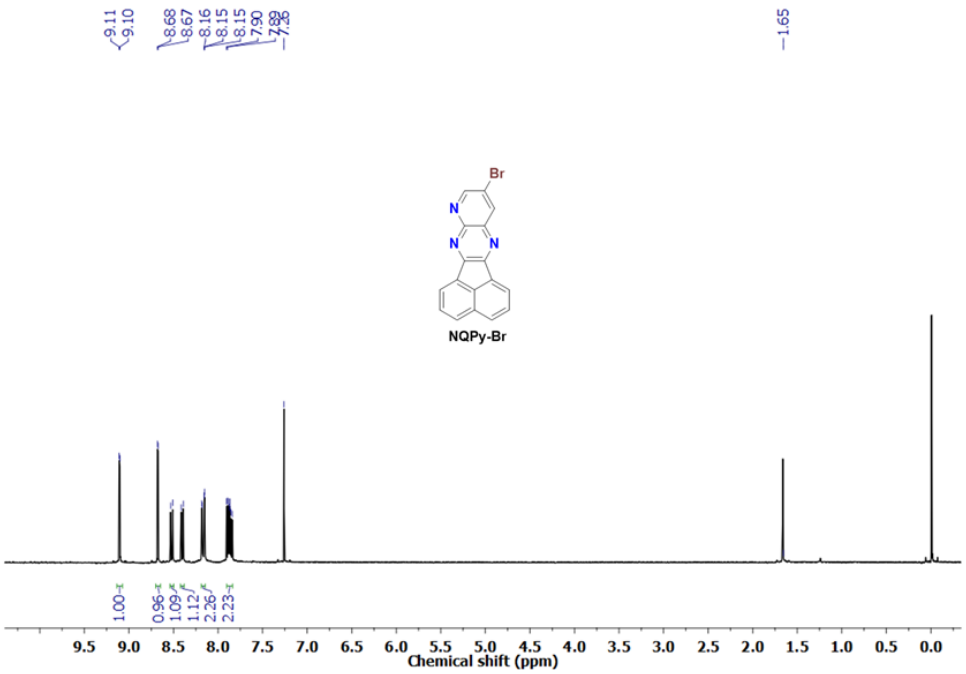

Figure S1 – ^{1}H NMR (300 MHz) in $CDCl_3$ of the compound **NQPy-Br**.

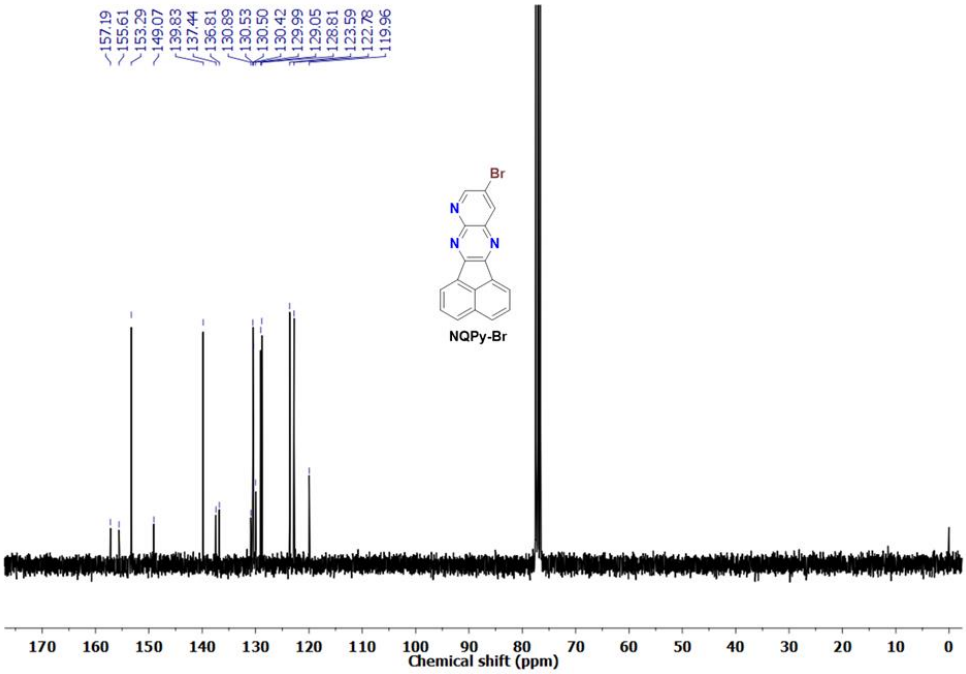

Figure S2 – ^{13}C NMR (75 MHz) in $CDCl_3$ of the compound **NQPy-Br**.

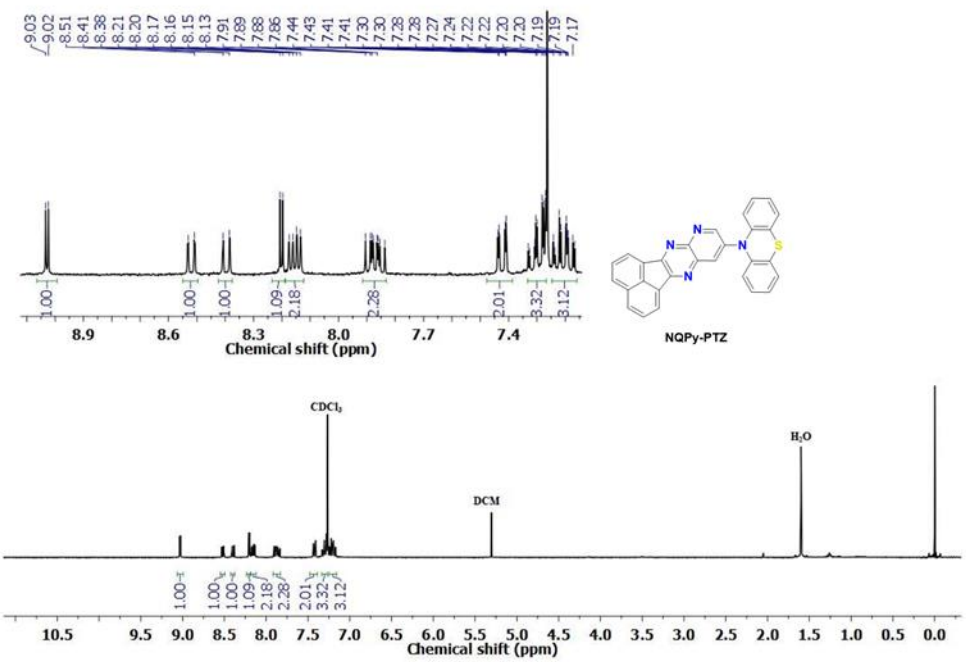

Figure S3 - ^{1}H NMR (300 MHz) in $CDCl_3$ of the compound **NQPy-PTZ**.

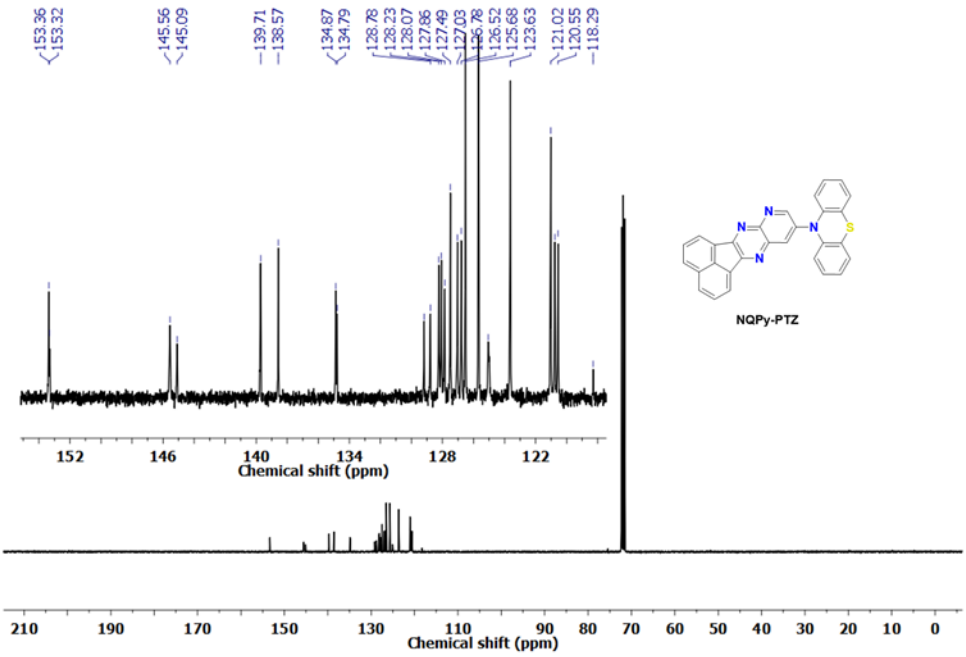

Figure S4 - ^{13}C NMR (75 MHz) in 1,1,2,2-Tetrachloroethane-d_2 of the compound **NQPy-PTZ**

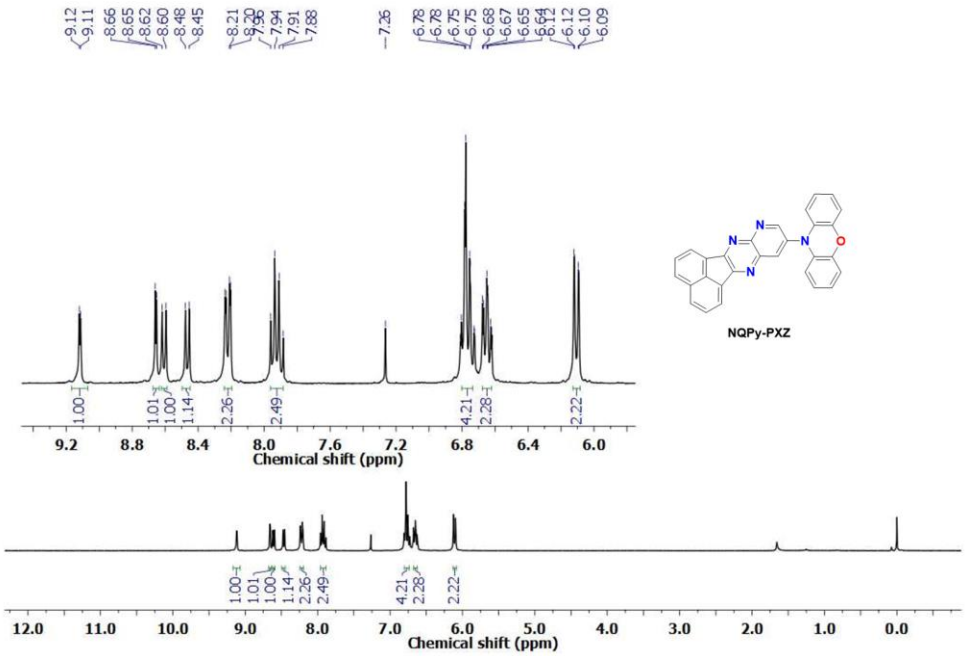

Figure S5 – ^{1}H NMR (300 MHz) in $CDCl_3$ of the compound **NQPy-PXZ.**

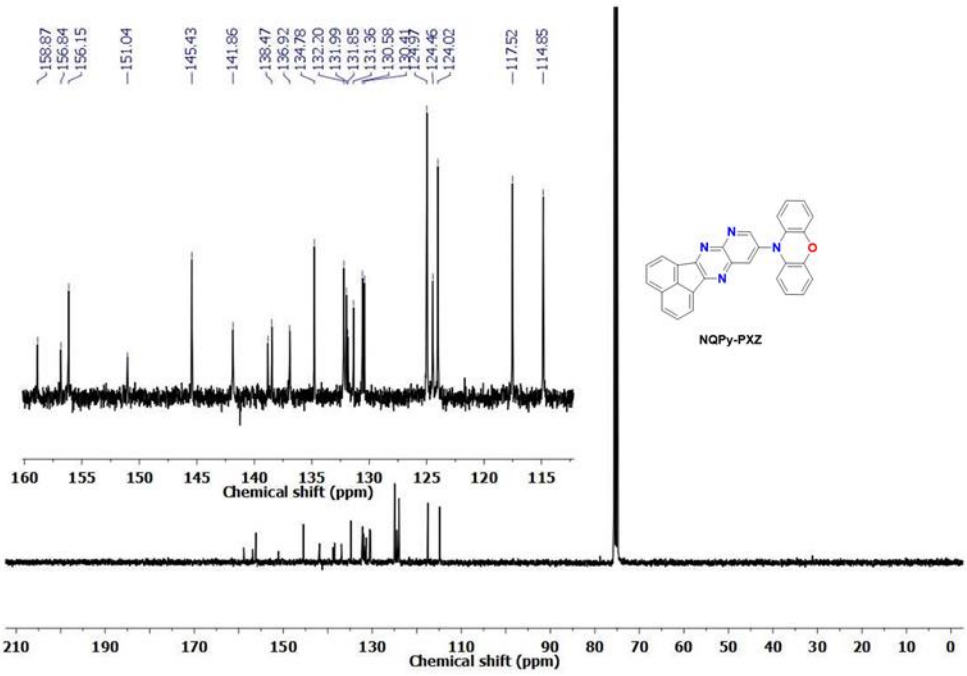

Figure S6 - ^{13}C NMR (75 MHz) in 1,1,2,2-Tetrachloroethane-d_2 of the compound **NQPy-PXZ**

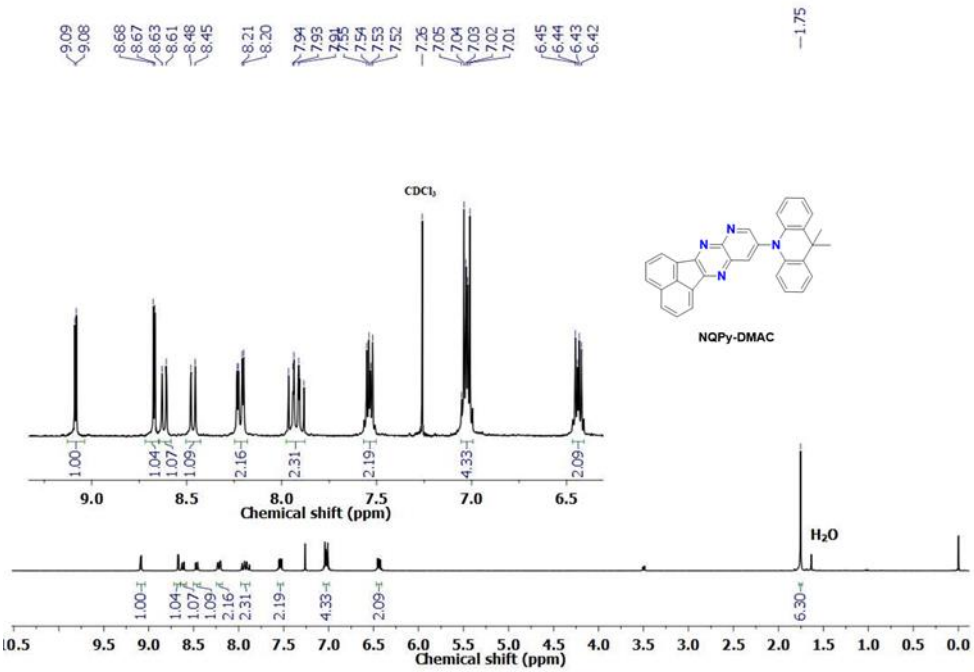

Figure S7 – ^{1}H NMR (300 MHz) in $CDCl_3$ of the compound **NQPy-DMAC**

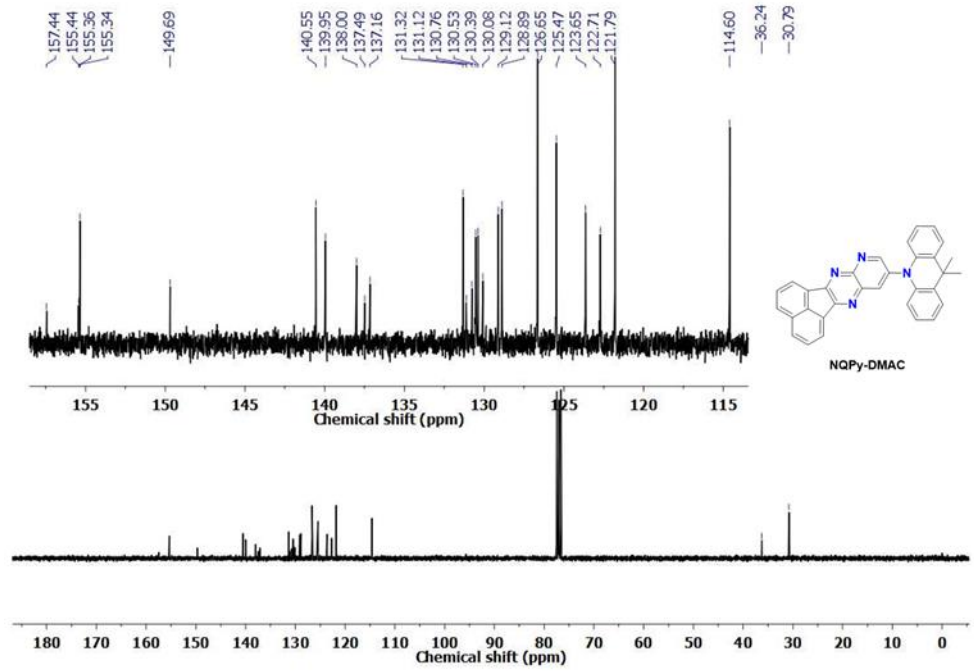

Figure S8 - ^{13}C NMR (75 MHz) in $CDCl_3$ of the compound **NQPy-DMAC**

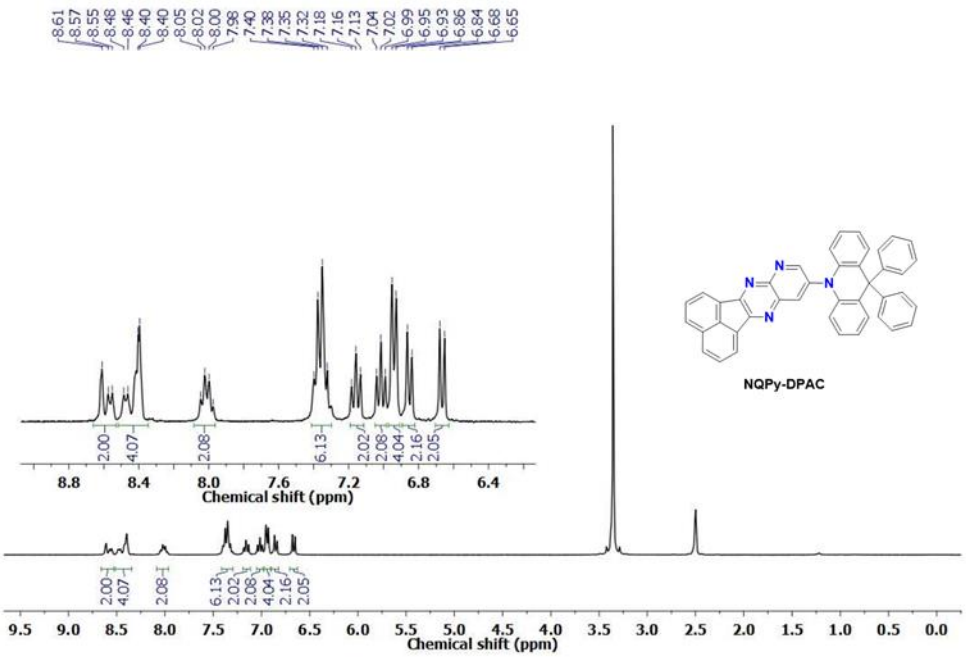

Figure S9 – ^{1}H NMR (300 MHz) in DMSO-d_6 of the compound **NQPy-DPAC**

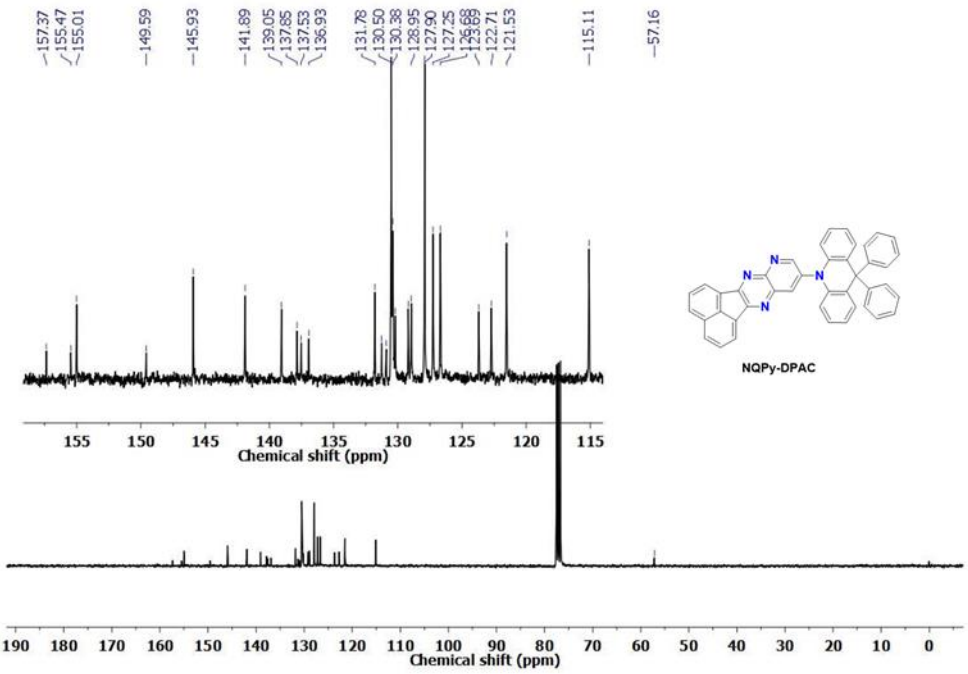

Figure S10 - ^{13}C NMR (75 MHz) in $CDCl_3$ of the compound **NQPy-DPAC**

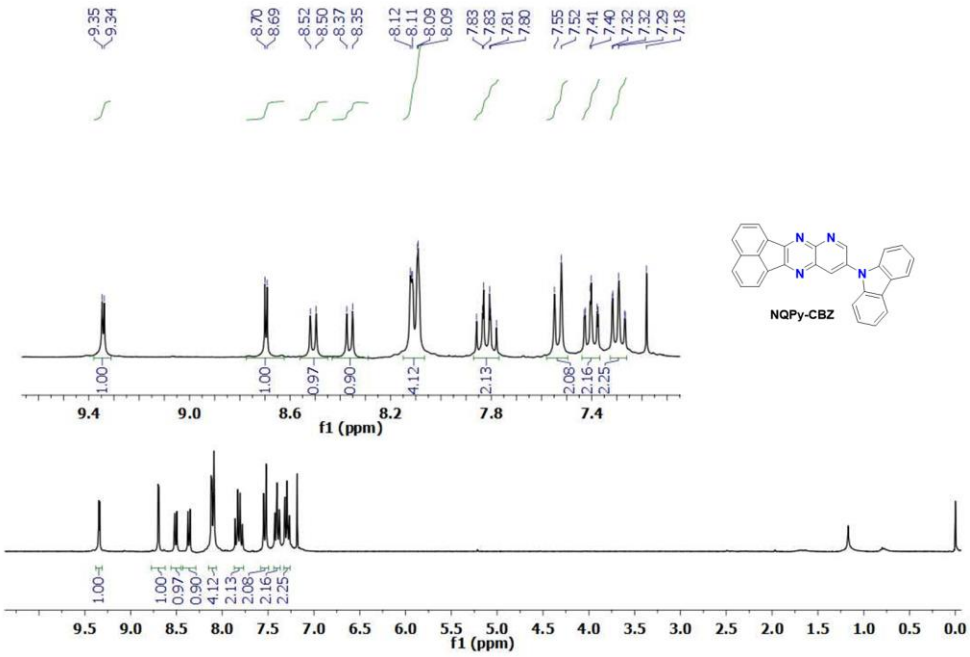

Figure S11 – ^{1}H NMR (300 MHz) in $CDCl_3$ of the compound **NQPy-CBZ**

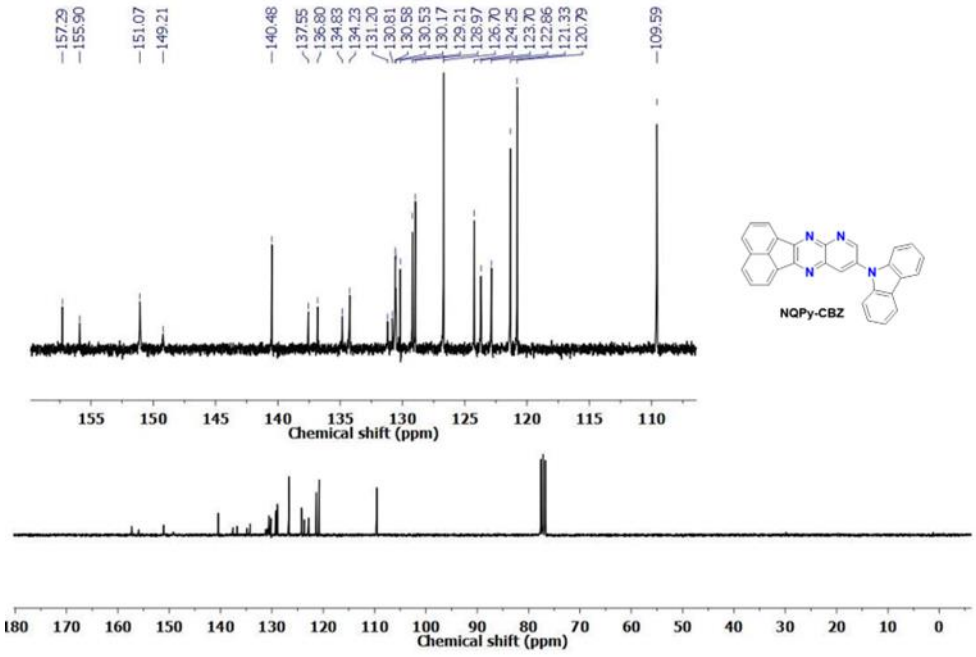

Figure S12 - ^{13}C NMR (75 MHz) in $CDCl_3$ of the compound **NQPy-CBZ**

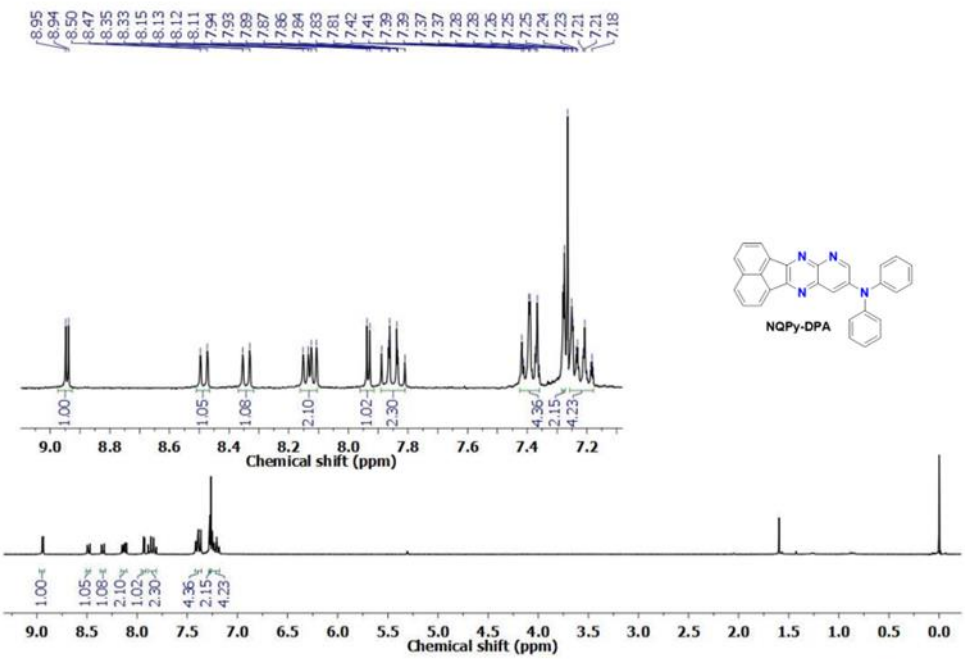

Figure S13 – ^{1}H NMR (300 MHz) in $CDCl_3$ of the compound **NQPy-DPA**

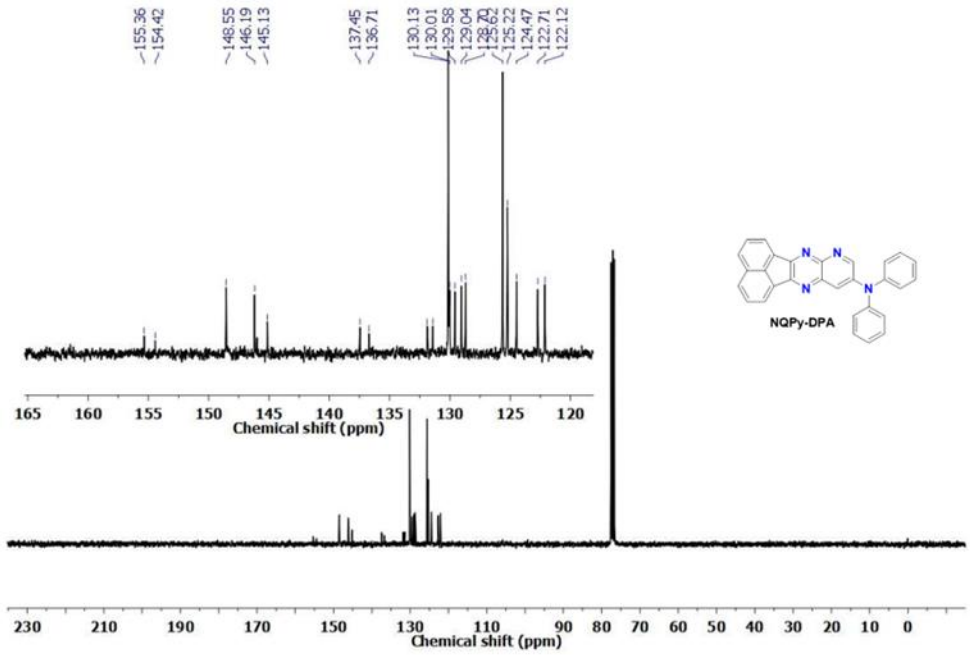

Figure S14 - ^{13}C NMR (75 MHz) in $CDCl_3$ of the compound **NQPy-DPA**

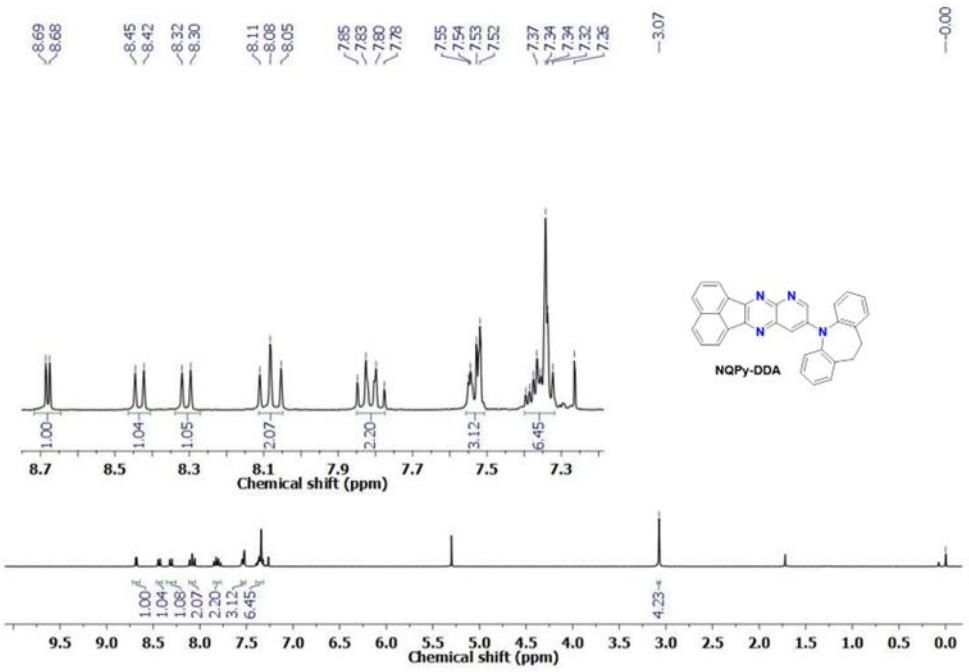

Figure S15 – ^{1}H NMR (300 MHz) in $CDCl_3$ of the compound **NQPy-DDA**

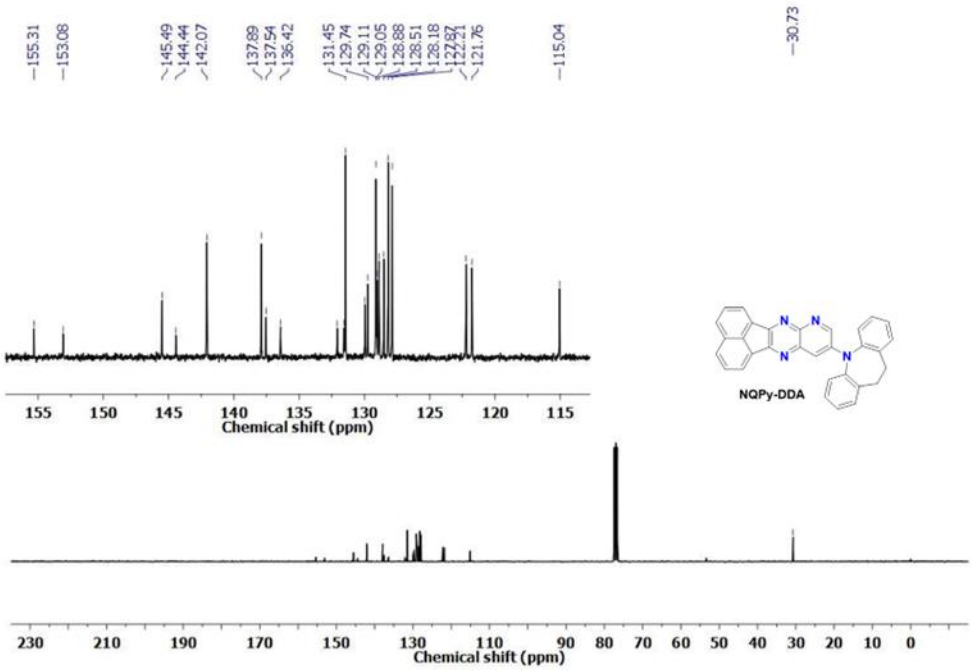

Figure S16 – ^{13}C NMR (75 MHz) in $CDCl_3$ of the compound **NQPy-DDA**

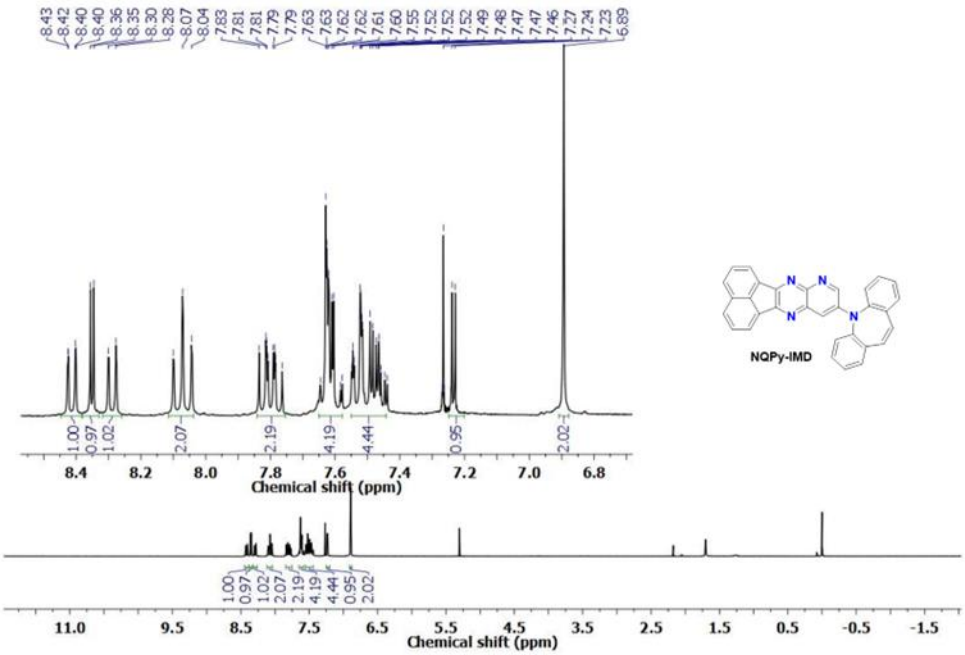

Figure S17 – ^{1}H NMR (300 MHz) in $CDCl_3$ of the compound **NQPy-IMD**

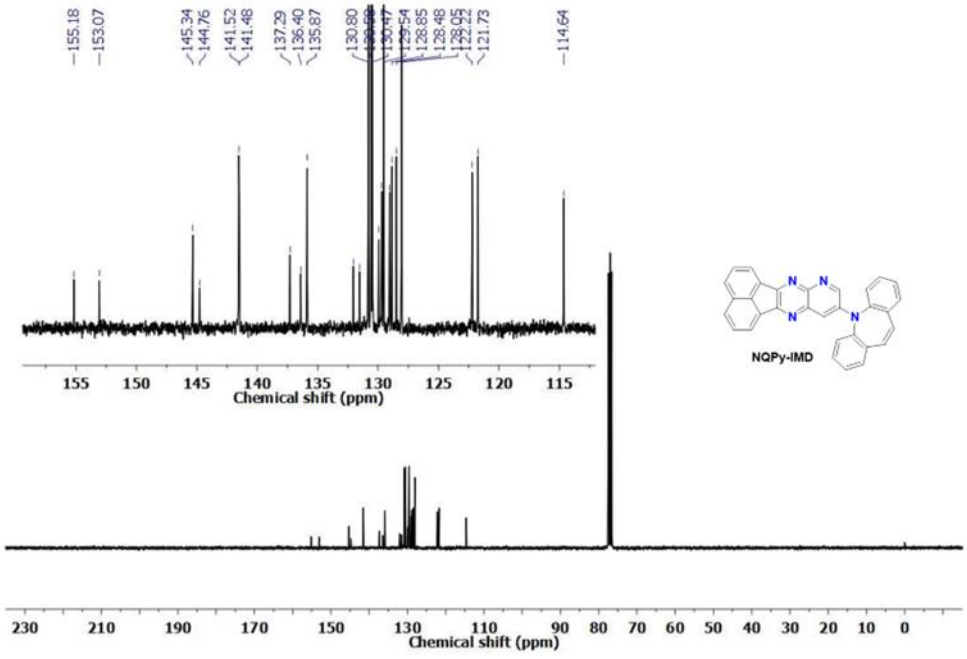

Figure S18 – ^{13}C NMR (75 MHz) in $CDCl_3$ of the compound **NQPy-IMD**

10. Additional theoretical data

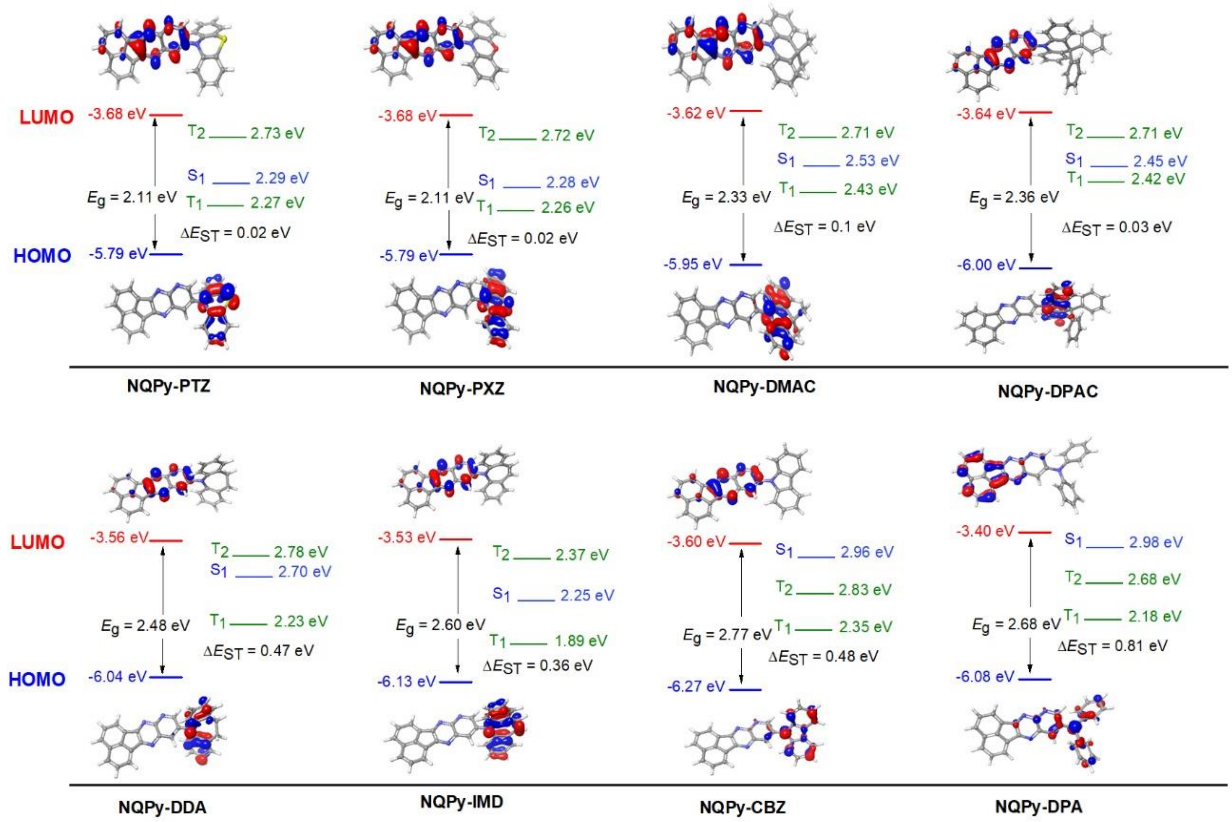

Figure S19 – HOMO and LUMO spatial distributions, energy of the S_1, T_1, and T_2 states as well as the ΔE_{ST} and energy gap (E_g) for the **NQPy-Donor** molecules using DFT and TD-DFT at the B3LYP/6-31G** level. Isovalue 0.03.

Table S1. Overlap between HOMO and LUMO calculated at the B3LYP/6-31G** level of theory using Multiwfn based on wavefunctions calculated with Orca 5.0.3.

	Overlap integral[a]
NQPy-PTZ	0.14
NQPy-PXZ	0.13
NQPy-DMAC	0.14
NQPy-DPAC	0.13
NQPy-DDA	0.21
NQPy-IMD	0.17
NQPy-CBZ	0.40
NQPy-DPA	0.39

[a] Overlap integral is a product of the following expression: $O = \int |\varphi_i| |\varphi_j| dr$, where φ_i, j are the wavefunctions of HOMO and LUMO, respectively.[5]

11. Additional cyclic voltammetry data

Table S2. HOMO and LUMO estimated values from the oxidation and reduction potentials.

	HOMO (eV)	LUMO (eV)	$E_{oxi\ onset}$ (V)	$E_{red\ onset}$ (V)
NQPy-PTZ	-5.49	-3.45	0.39	-1.65
NQPy-PXZ	-5.56	-3.56	0.46	-1.54
NQPy-DMAC	-5.68	-3.44	0.58	-1.66
NQPy-DPAC	-5.77	-3.44	0.67	-1.66
NQPy-DDA	-5.90	-3.19	0.80	-1.91
NQPy-IMD	-5.87	-3.18	0.77	-1.92
NQPy-CBZ	-6.01	-3.49	0.91	-1.61
NQPy-DPA	-5.85	-3.41	0.75	-1.69

We used a scan rate of 100 mV s^{-1} and HOMO and LUMO were estimated assuming the ionization potential of ferrocene equal to -5.1 eV and using the formula: $E_{HOMO\ or\ LUMO} = -(5.1 + E_{oxi\ or\ red\ onset})$.[6,7]

12. Additional photophysical data

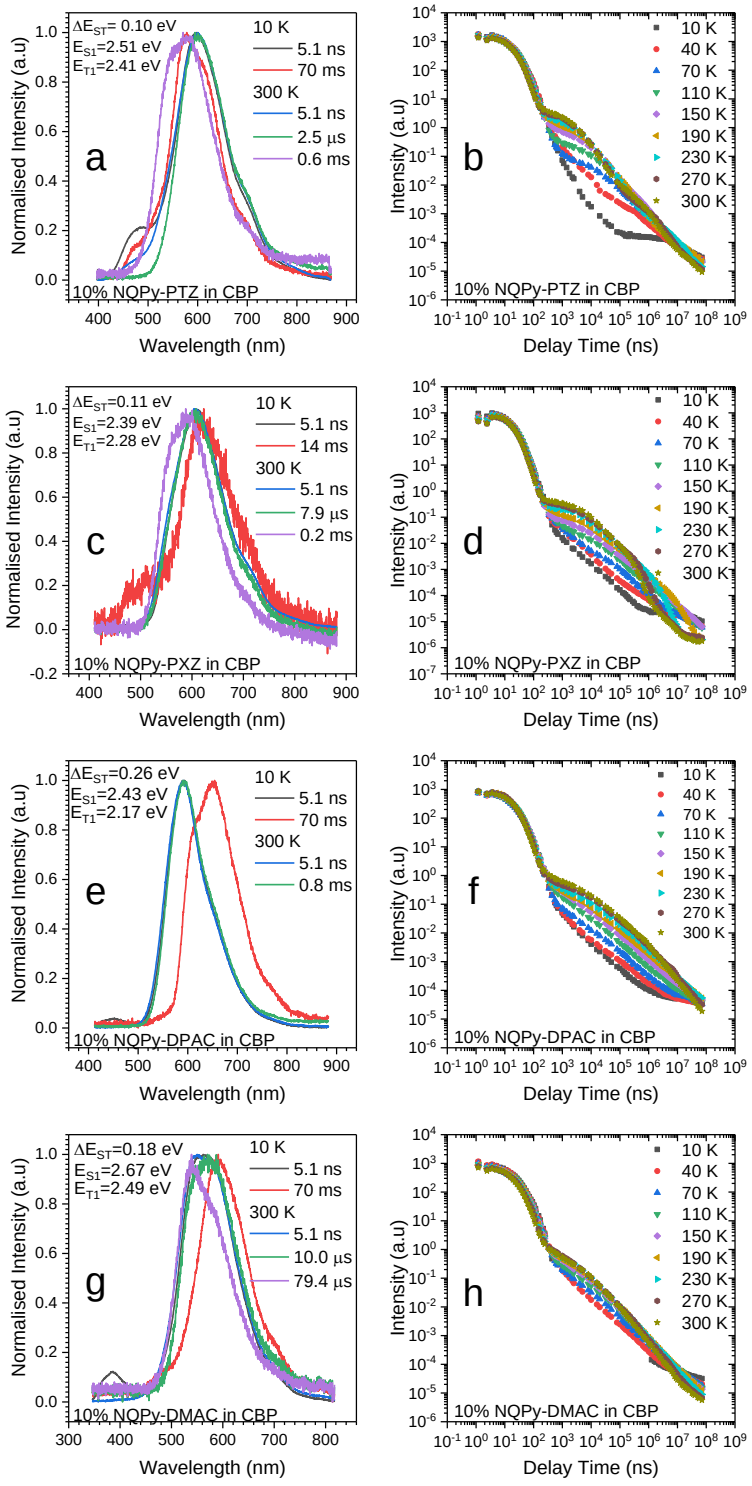

Figure S20 – Time-Resolved spectra and the intensity *vs*. delay time measurements of **NQPy-PTZ**, **NQPy-PXZ**, **NQPy-DPAC** and **NQPy-DMAC** compounds 10 wt% in CBP matrix.

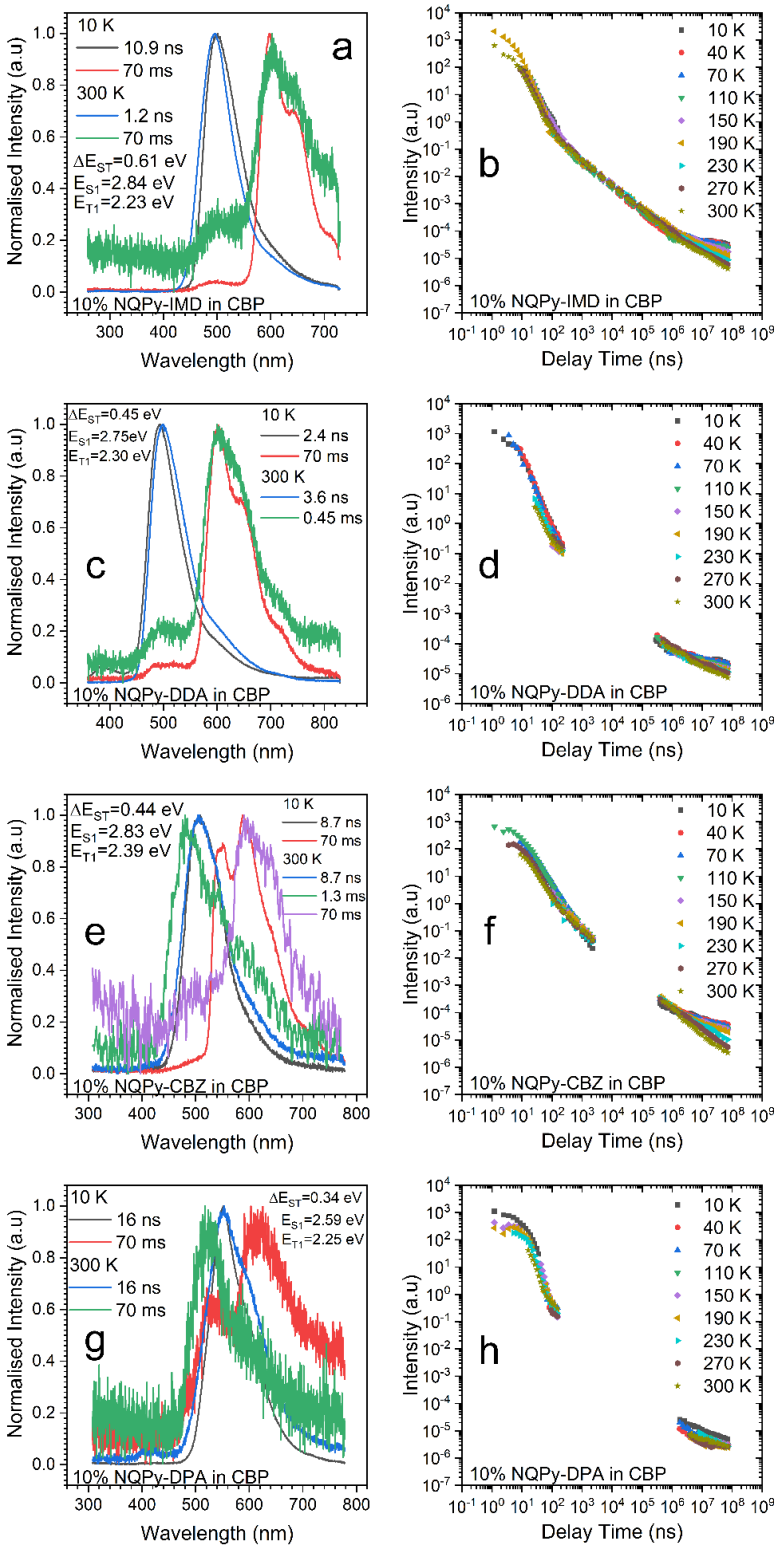

Figure S21 – Time-Resolved spectra and the intensity *vs*. delay time measurements of **NQPy-IMD**, **NQPy-DDA**, **NQPy-CBZ** and **NQPy-DPA** compounds 10 wt% in CBP matrix. matrix.

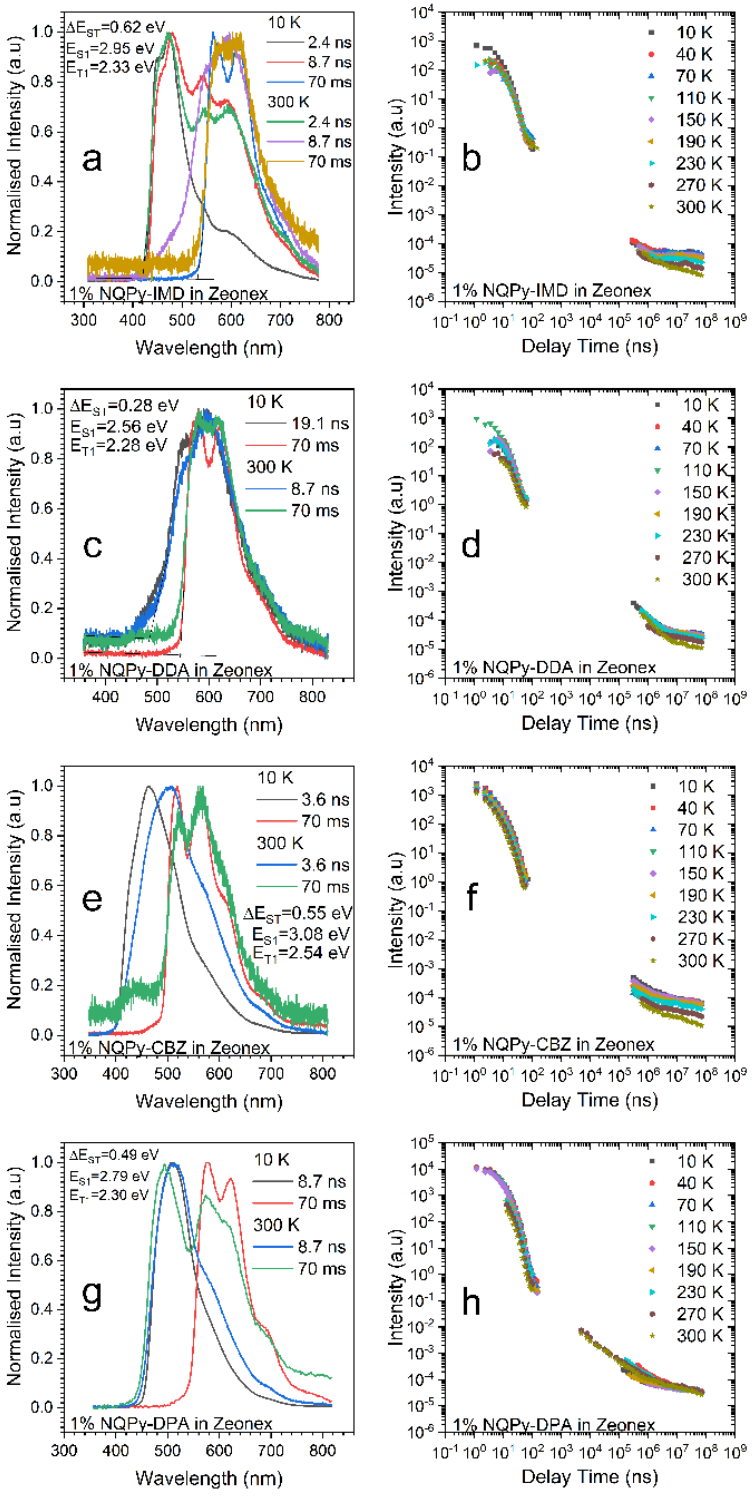

Figure S22. Time-Resolved spectra and the intensity *vs*. delay time measurements of **NQPy-IMD, NQPy-DDA, NQPy-CBZ and NQPy-DPA** compounds 1 wt% in Zeonex matrix.

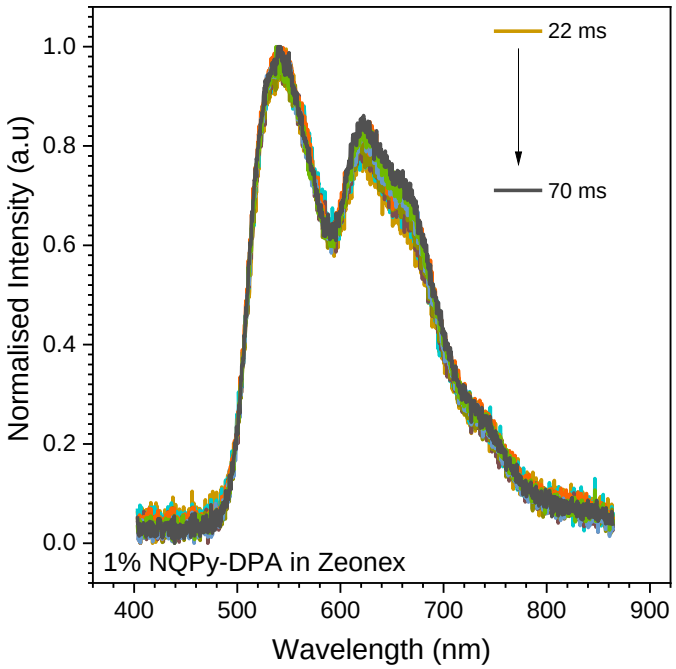

Figure S23. Normalized time resolved spectra at 300 K from 22 ms to 70 ms for 1% of **NQPy-DPA** in Zeonex matrix.

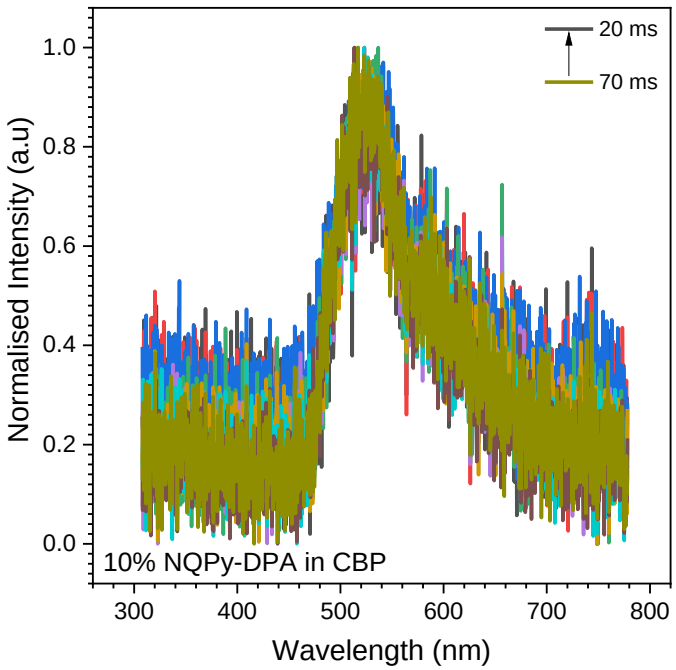

Figure S24. Normalized time resolved spectra at 300 K from 20 ms to 70 ms for 10% of **NQPy-DPA** in CBP matrix.

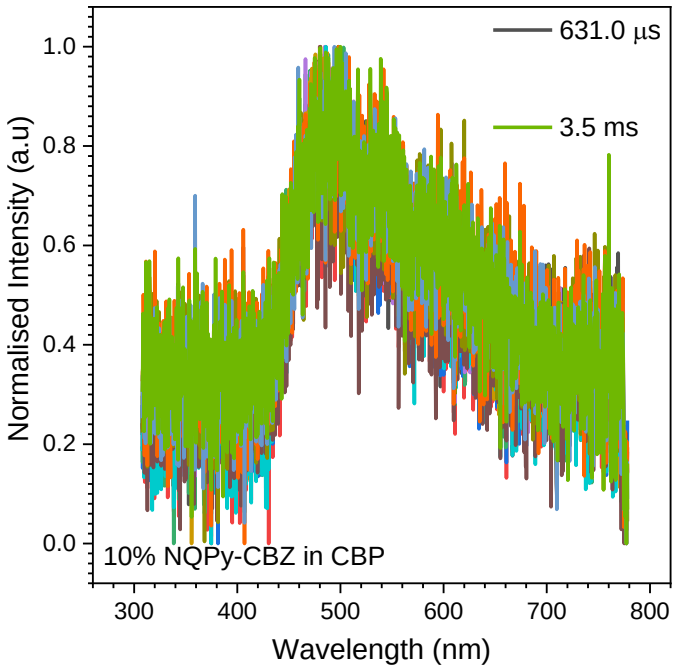

Figure S25. Normalized time resolved spectra at 300 K from 631.0 µs to 3.5 ms for 10% of **NQPy-CBZ** in CBP matrix.

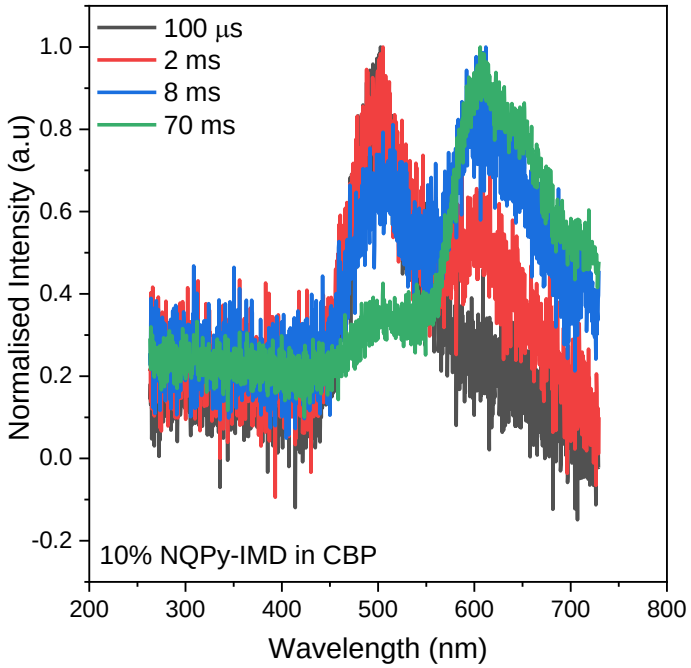

Figure S26. Normalized time resolved spectra at 300 K at 100 µs, 2 ms, 8 ms and 70 ms for 10% of **NQPy-IMD** in CBP matrix.

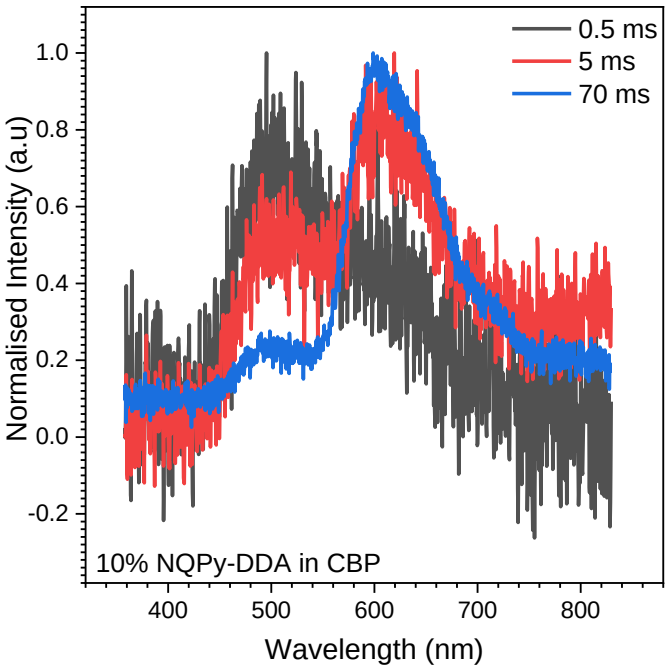

Figure S27. Normalized time resolved spectra at 300 K at 0.5 ms, 5 ms and 70 ms for 10% of **NQPy-DDA** in CBP matrix.

13. Singlet oxygen generation

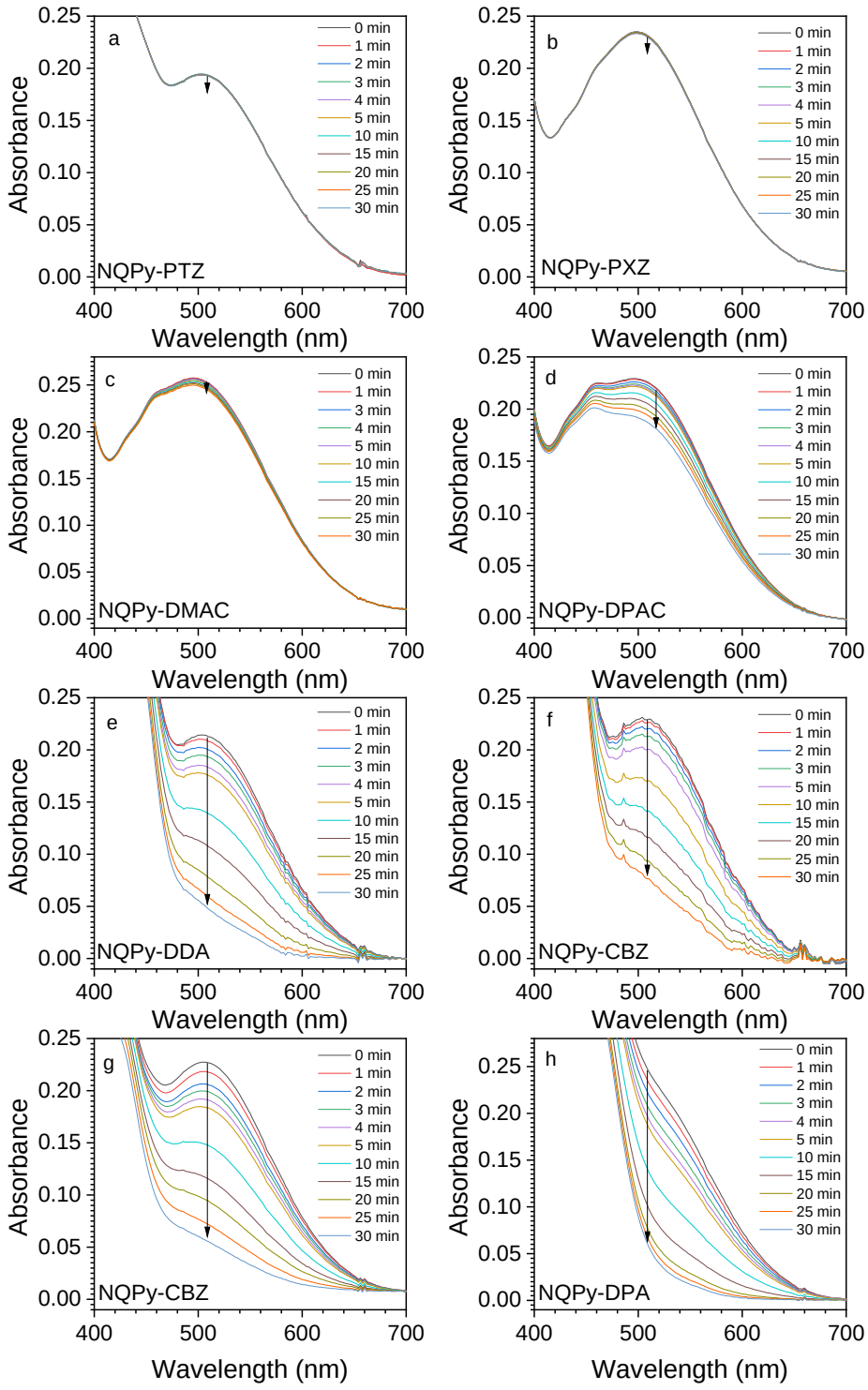

Figure S28. Absorption spectra of photosensitizers and TPCPD in DCM recorded while irradiating the sample using a 445 nm laser in the timescale from 0 up to 100 min.

14. Aggregation study

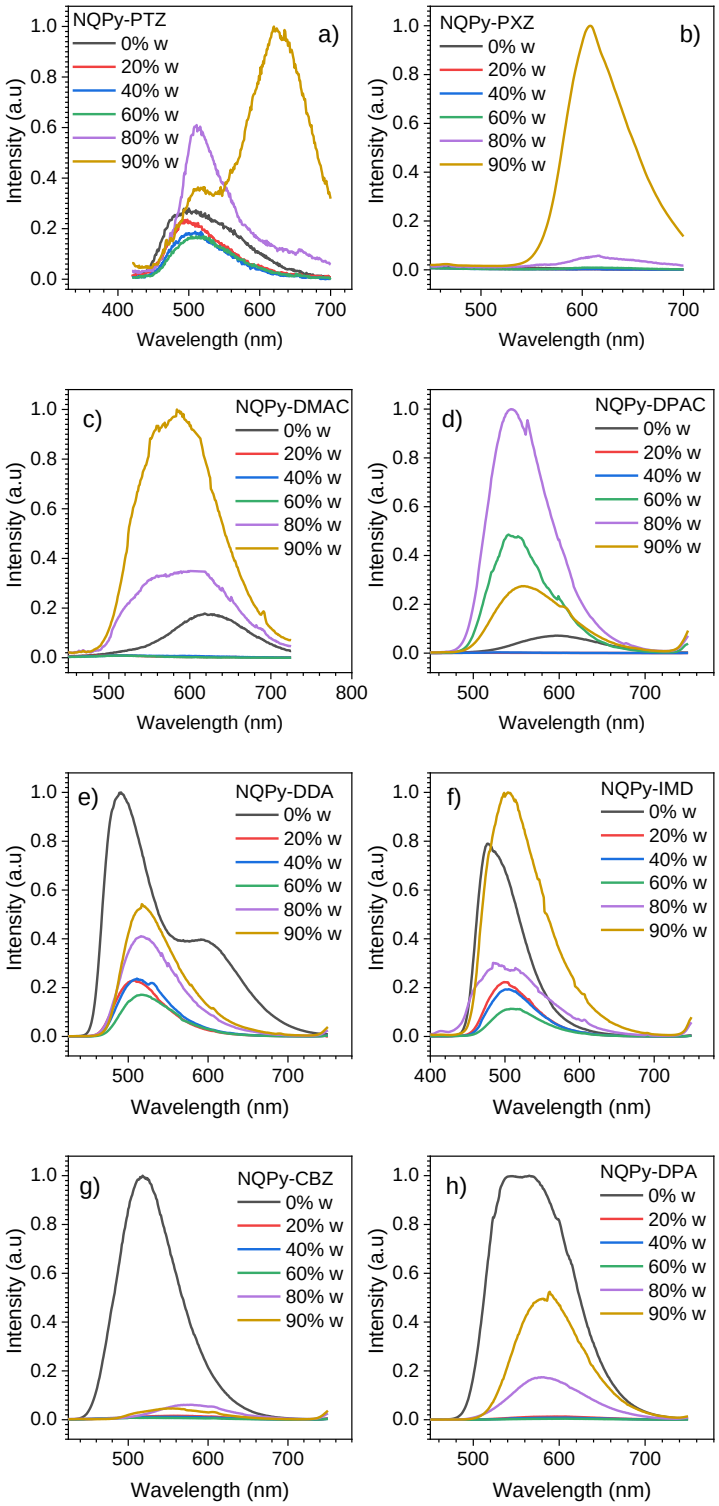

Figure S29. Emission spectra recorded in THF/water mixtures for water fractions f_w = 0-90%.

Table S3. The increase obtained for the emission of the aggregates in Water/THF solutions.

	NQPy-PTZ	NQPy-PXZ	NQPy-DMAC	NQPy-DPAC	NQPy-DDA	NQPy-IMD	NQPy-CBZ	NQPy-DPA
INCREASE 1	5.9	116.2	336.0	879.4	2.4	8.9	6.5	120.3
INCREASE 2	3.6	52.5	5.6	14.0	0.5	1.3	0.1	0.5

Increase 1 is relative to the increase after the maximum quenching (the less emissive curve). Increase 2 is relative to the increase in relation to 0% water (pure THF).

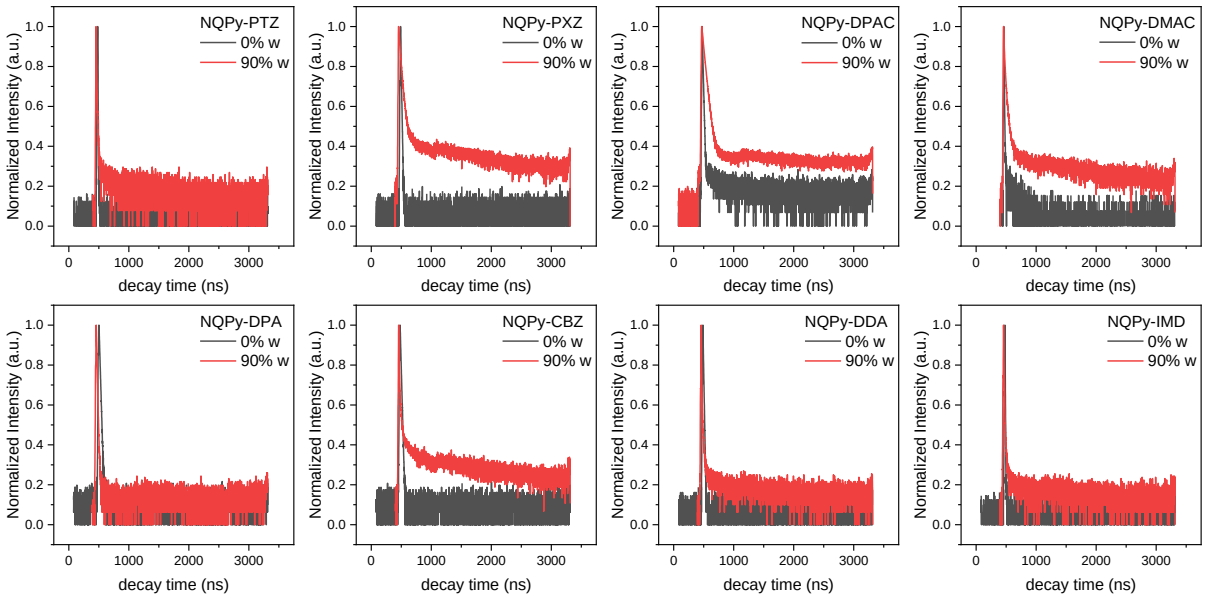

Figure S30. TCSPC traces for 0 and 90% f_w in air-equilibrated solutions.

15. OLED devices additional data

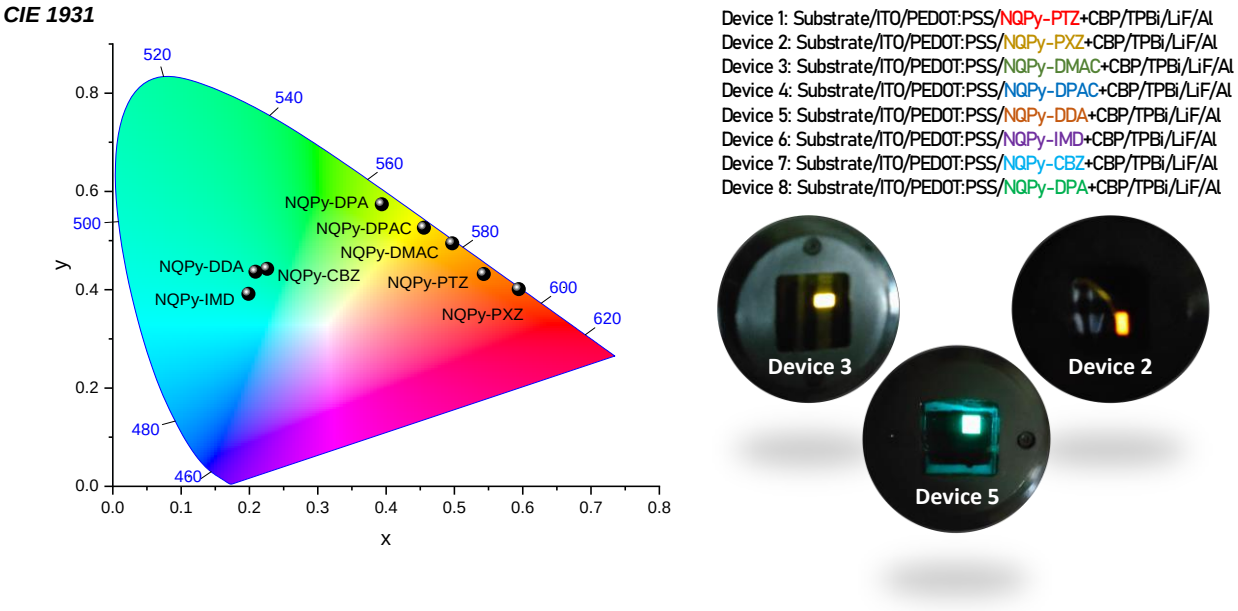

Figure S31. CIE 1931 diagram chromatic coordinates for NQPy-Donors electroluminescence in the devices 1-8.

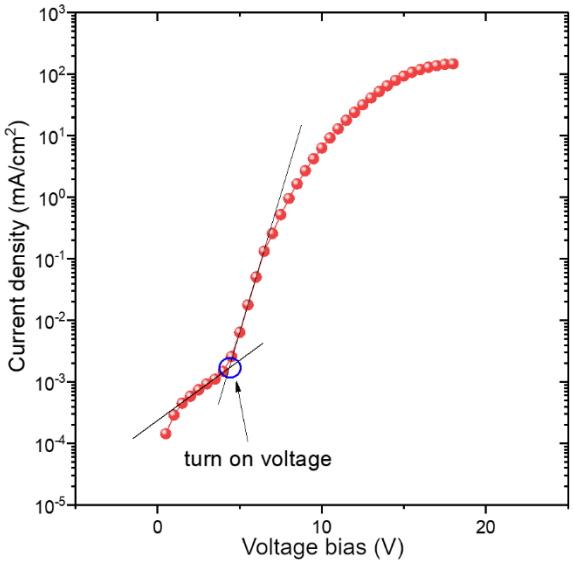

Figure S32. This figure demonstrates the methodology we used to determine the electrical turn-on voltage of OLEDs in this study.

16. Thermogravimetric analysis (TGA)

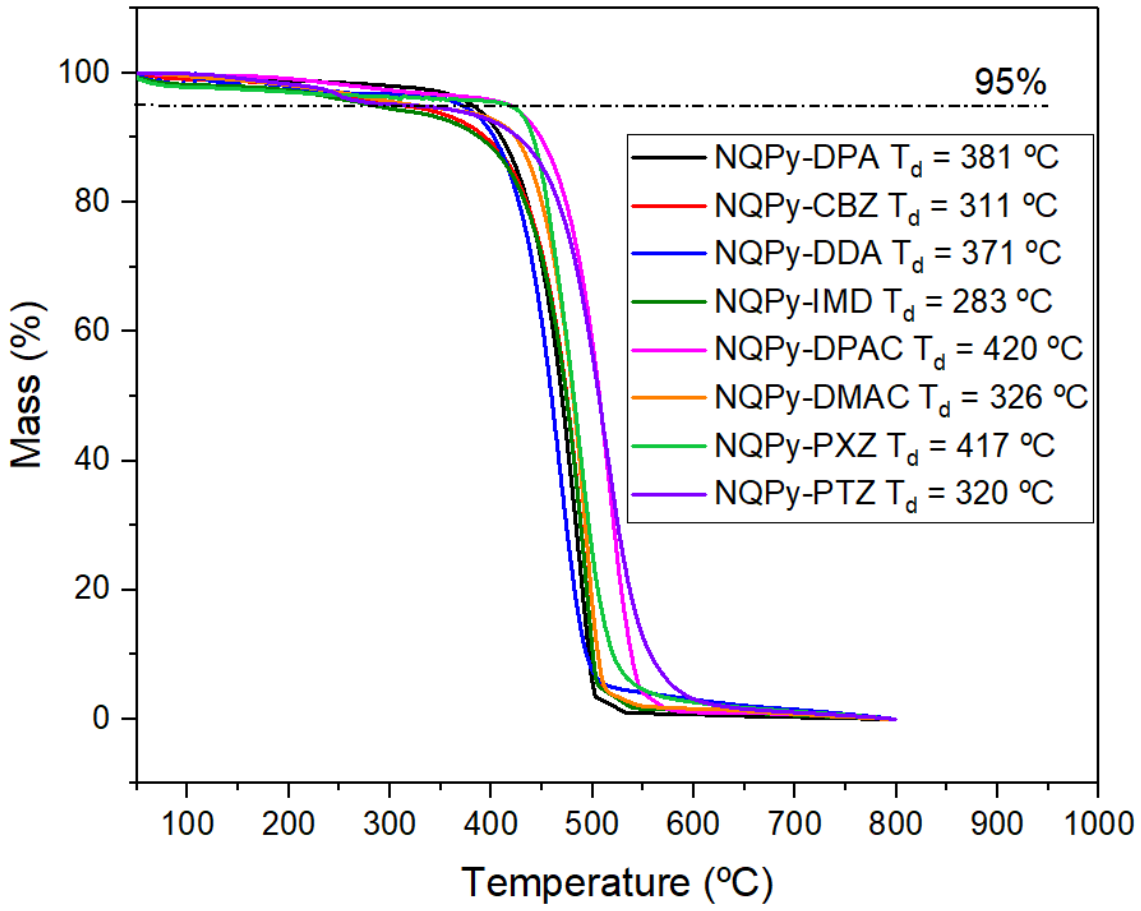

Figure S33. TGA traces recorded under nitrogen atmosphere (10 °C·min^{-1}) for all NQPy-donor molecules presented in this work. Decomposition temperatures (T_d) recorded at 5% of weight loss are presented alongside compound codes in the figure legend.

17. References

1 T. Goya, P. Zimmermann Crocomo, T. Hosono, S. Minakata, L. E. de Sousa, P. de Silva, P. Data and Y. Takeda, *Asian J. Org. Chem.*, 2022, **11**, 1–7.

2 S. S. Reddy, V. G. Sree, K. Gunasekar, W. Cho, Y. S. Gal, M. Song, J. W. Kang and S. H. Jin, *Adv. Opt. Mater.*, 2016, **4**, 1236–1246.

3 R. Schmidt, C. Tanielian, R. Dunsbach and C. Wolff, *J. Photochem. Photobiol. A Chem.*, 1994, **79**, 11–17.

4 R. Motyka, K. Nastula, P. Pander, D. Honisz, M. Tomczyk, K. Erfurt and A. Blacha-Grzechnik, *Materials (Basel).*, 2023, **16**, 2605.

5 T. J. Penfold, *J. Phys. Chem. C*, 2015, **119**, 13535–13544.

6 M. Matussek, A. Kurpanik-Wójcik, S. Gogoc, A. Fijołek, M. Filapek, B. Naumczuk and P. Data, *Chem. – A Eur. J.*, 2023, e202302115.

7 C. M. Cardona, W. Li, A. E. Kaifer, D. Stockdale and G. C. Bazan, *Adv. Mater.*, 2011, **23**, 2367–2371.